IOPscience iopscience.iop.org

Home Search Collections Journals About Contact us My IOPscience

Inter-band magnetoplasmons in mono- and bilayer graphene

This article has been downloaded from IOPscience. Please scroll down to see the full text article.

2008 J. Phys.: Condens. Matter 20 425202

(http://iopscience.iop.org/0953-8984/20/42/425202)

View the table of contents for this issue, or go to the journal homepage for more

Download details:
IP Address: 129.252.86.83
The article was downloaded on 29/05/2010 at 15:58

Please note that terms and conditions apply.

J. Phys.: Condens. Matter **20** (2008) 425202 (5pp) doi:10.1088/0953-8984/20/42/425202

Inter-band magnetoplasmons in mono- and bilayer graphene

M Tahir[1,3] **and K Sabeeh**[2]

[1] Department of Physics, University of Sargodha, Sargodha, Pakistan
[2] Department of Physics, Quaid-i-Azam University, Islamabad, Pakistan

E-mail: mtahir06@imperial.ac.uk, ksabeeh@qau.edu.pk and kashifsabeeh@hotmail.com

Received 5 May 2008, in final form 23 July 2008
Published 9 September 2008
Online at stacks.iop.org/JPhysCM/20/425202

Abstract
Collective excitation spectra of Dirac electrons in mono- and bilayer graphene in the presence of a uniform magnetic field are investigated. Analytical results for inter-Landau-band plasmon spectra within the self-consistent-field approach are obtained. Shubnikov–de Haas (SdH) type oscillations that are a monotonic function of the magnetic field are observed in the plasmon spectrum of both mono- and bilayer graphene systems. The results presented are also compared with those obtained in a conventional two-dimensional electron gas (2DEG). The chiral nature of the quasiparticles in mono- and bilayer graphene systems results in the observation of π and 2π Berry's phase in the SdH-type oscillations in the plasmon spectrum.

1. Introduction

Recent progress in the experimental realization of both monolayer and bilayer graphene has led to extensive exploration of the electronic properties in these systems [1, 2]. Experimental and theoretical studies have shown that the nature of quasiparticles in these two-dimensional systems is very different from those of the conventional two-dimensional electron gas (2DEG) systems realized in semiconductor heterostructures. Graphene has a honeycomb lattice of carbon atoms. The quasiparticles in monolayer graphene have a band structure in which electron and hole bands touch at two points in the Brillouin zone. At these Dirac points the quasiparticles obey the massless Dirac equation, leading to a linear dispersion relation $\epsilon_k = v_F k$ (with the Fermi speed $v_F = 10^6$ m s^{-1}). This difference in the nature of the quasiparticles in monolayer graphene from conventional 2DEG has given rise to a host of new and unusual phenomena such as the anomalous quantum Hall effects and a π Berry phase [1, 2]. These transport experiments have shown results in agreement with the presence of Dirac fermions. The 2D Dirac-like spectrum was confirmed recently by cyclotron resonance measurements and also by angle resolved photoelectron spectroscopy (ARPES) measurements in monolayer graphene [3]. Recent theoretical work on graphene multilayers has also shown the existence of Dirac electrons with a linear energy spectrum in monolayer graphene [4]. On the other hand, experimental and theoretical results have shown that quasiparticles in bilayer graphene exhibit a parabolic dispersion relation and they can not be treated as massless but have a finite mass. In addition, The quasiparticles in both the graphene systems are chiral [2, 4–7].

Plasmons are a very general phenomena and have been studied extensively in a wide variety of systems including ionized gases, simple metals and semiconductor 2DEG systems. In a 2DEG, these collective excitations are induced by the electron–electron interactions. Collective excitations (plasmons) are among the most important electronic properties of a system. In the presence of an external magnetic field, these collective excitations are known as magnetoplasmons. Magnetic oscillations of the plasmon frequency occur in a magnetic field. Single particle magneto-oscillatory phenomena such as the Shubnikov–de Haas (SdH) and de Haas–van Alphen effects have provided very important probes of the electronic structure of solids. Their collective analogue yields important insight into collective phenomena [8–15]. Collective excitations of Dirac electrons in monolayer and bilayer graphene in the absence of a magnetic field have been investigated [16–20]. Magnetic field effects on the plasmon spectrum have not been studied so far. In addition, since the quasiparticles in graphene are chiral, the particles will acquire Berry's phase as they move in the magnetic field leading to observable effects on the plasmon spectrum. To this end, in the present work, we study the magnetoplasmon spectrum within the self-consistent-field approach for both the monolayer and

[3] Present address: Department of Physics, Blackett Laboratory, Imperial College London, London SW7 2AZ, UK.

 © 2008 IOP Publishing Ltd Printed in the UK

bilayer graphene systems. Magnetoplasmons can be observed by inelastic light scattering experiments as revealed in studies carried out on 2DEG systems [11–15]. Similarly, inelastic light scattering experiments are expected to yield information about the magnetoplasmons in graphene. Furthermore, the results presented here can also be experimentally observed by electron energy loss spectroscopy (EELS) on graphene [21].

2. Electron energy spectrum in monolayer graphene

We consider Dirac electrons in graphene moving in the x–y-plane. The magnetic field (B) is applied along the z-direction perpendicular to the graphene plane. We employ the Landau gauge and write the vector potential as $A = (0, Bx, 0)$. The two-dimensional Dirac-like Hamiltonian for a single electron in the Landau gauge is ($\hbar = c = 1$ here) [1, 2]

$$H_0 = v_{\mathrm{F}}\sigma \cdot (-\mathrm{i}\nabla + eA). \tag{1}$$

Here $\sigma = \{\sigma_x, \sigma_y\}$ are the Pauli matrices and v_{F} characterizes the electron Fermi velocity. The energy eigenfunctions are given by

$$\Psi_{n,k_y}(r) = \frac{\mathrm{e}^{\mathrm{i}k_y y}}{\sqrt{2L_y l}} \begin{pmatrix} -\mathrm{i}\Phi_{n-1}[(x + x_0)/l] \\ \Phi_n[(x + x_0)/l] \end{pmatrix} \tag{2}$$

where

$$\Phi_n(x) = \frac{\mathrm{e}^{-x^2/2}}{\sqrt{2^n n!\sqrt{\pi}}} H_n(x),$$

$l = \sqrt{1/eB}$ is the magnetic length, $x_0 = l^2 k_y$, L_y is the y-dimension of the graphene layer and $H_n(x)$ are the Hermite polynomials. The energy eigenvalues are

$$\varepsilon(n) = \omega_{\mathrm{g}}\sqrt{n} \tag{3}$$

where $\omega_{\mathrm{g}} = v\sqrt{2eB}$ is the cyclotron frequency of the monolayer graphene and n is an integer. Note that the Landau level spectrum for Dirac electrons is significantly different from the spectrum for electrons in a conventional 2DEG which is given as $\varepsilon(n) = \hbar\omega_{\mathrm{c}}(n + 1/2)$. The Landau level spectrum in graphene has a $\sqrt{n}$ dependence on the Landau level index as against the linear dependence in a 2DEG. The monolayer graphene has four-fold degenerate (spin and valley) states with the $n = 0$ level having energy $\varepsilon(n = 0) = 0$. The quasiparticles in this system are chiral, exhibiting π Berry's phase.

3. Electron energy spectrum for bilayer graphene

The Landau level energy eigenvalues and eigenfunctions are given by [5]

$$\varepsilon(n) = \omega_{\mathrm{b}}\sqrt{n(n-1)}, \tag{4}$$

$$\Psi^{\pm}_{n,K} = \frac{1}{\sqrt{2}} \begin{pmatrix} \Phi_n \\ \pm\Phi_{n-2} \\ 0 \\ 0 \end{pmatrix}, \tag{5}$$

$$\Psi^{\pm}_{n,K'} = \frac{1}{\sqrt{2}} \begin{pmatrix} 0 \\ 0 \\ \pm\Phi_{n-2} \\ \Phi_n \end{pmatrix}, \tag{6}$$

where $\pm$ are assigned to electron and hole states, $\omega_{\mathrm{b}} = \frac{eB}{m^*}$ is the cyclotron frequency of electrons in bilayer graphene and m^* is the effective mass given as $0.044m_{\mathrm{e}}$ with m_{e} being the bare electron mass. The Landau level spectrum of electrons given by equation (4) is distinctly different from that of monolayer graphene and a conventional 2DEG system. The electrons in the bilayer are quasiparticles that exhibit parabolic dispersion with a smaller effective mass than the standard electrons. Bilayer graphene has four-fold degenerate (spin and valley) states other than the $n = 0$ level with energy $\varepsilon(n = 0) = 0$ which is eight-fold degenerate. These quasiparticles are chiral, exhibiting 2π Berry's phase.

3.1. Inter-Landau-band plasmon spectrum of monolayer and bilayer graphene in a magnetic field

The dynamic and static response properties of an electron system are all embodied in the structure of the density–density correlation function. We employ the Ehrenreich–Cohen self-consistent-field (SCF) approach [22] to calculate the density–density correlation function. The SCF treatment presented here is by its nature a high density approximation which has been successfully employed in the study of collective excitations in low-dimensional systems both with and without an applied magnetic field. It has been found that SCF predictions of plasmon spectra are in excellent agreement with experimental results. Following the SCF approach, one can express the dielectric function as

$$\epsilon(\bar{q}, \omega) = 1 - v_{\mathrm{c}}(\bar{q})\Pi(\bar{q}, \omega), \tag{7}$$

where the two-dimensional Fourier transform of the Coulomb potential $v_{\mathrm{c}}(\bar{q}) = \frac{2\pi e^2}{\kappa\bar{q}}$, $\bar{q} = (q_x^2 + q_y^2)^{1/2}$, κ is the background dielectric constant and $\Pi(\bar{q}, \omega)$ is the non-interacting density–density correlation function

$$\Pi(\bar{q}, \omega) = \frac{2}{\pi l^2} \sum C_{nn'}\left(\frac{\bar{q}^2}{2eB}\right)[f(\varepsilon(n) - f(\varepsilon(n'))] \times [\varepsilon(n) - \varepsilon(n') + \omega + \mathrm{i}\eta]^{-1}, \tag{8}$$

where $C_{nn'}(x) = (n_2!/n_1!)(x)^{n_1-n_2}\mathrm{e}^{-x}[L_{n_2}^{n_1-n_2}(x)]^2$ with $n_1 = \max(n, n')$, $n_2 = \min(n, n')$, $L_n^l(x)$ an associated Laguerre polynomial with $x = \frac{\bar{q}^2}{2eB}$ here. This is a convenient form of $\Pi(\bar{q}, \omega)$ that facilitates writing of the real and imaginary parts of the correlation function. The plasmon modes are determined from the roots of the longitudinal dispersion relation

$$1 - v_{\mathrm{c}}(\bar{q})\,\mathrm{Re}\,\Pi(\bar{q}, \omega) = 0 \tag{9}$$

along with the condition $\mathrm{Im}\,\Pi(\bar{q}, \omega) = 0$ to ensure long-lived excitations. Employing equations (8) and (9) gives

$$1 = \frac{2\pi e^2}{\kappa\bar{q}}\frac{2}{\pi l^2}\sum_{n,n'} C_{nn'}(x)\,(I_1(\omega) + I_1(-\omega)), \tag{10}$$

$$I_1(\omega) = \left(\frac{f(\varepsilon(n))}{\varepsilon(n) - \varepsilon(n') + \omega}\right), \tag{11}$$

and the factor of 2 is due to valley degeneracy. The plasmon modes originate from two kinds of electronic transitions: those involving different Landau bands (inter-Landau-band plasmons) and those within a single Landau-band (intra-Landau-band plasmons). Inter-Landau-band plasmons involve the local 2D magnetoplasma mode and the Bernstein-like plasma resonances, all of which involve excitation frequencies greater than the Landau-band separation. Since, in this work, we are not considering Landau level broadening only the inter-Landau-band plasmons will be investigated.

We now examine the inter-Landau-band transitions. In this case $n \neq n'$ and equation (11) yields

$$I_1(\omega) = \frac{f(\varepsilon(n))}{(\omega - \Delta)}, \tag{12}$$

where $\Delta = (\varepsilon(n) - \varepsilon(n'))$ which permits us to write the following term in equation (10) as

$$(I_1(\omega) + I_1(-\omega)) = 2\frac{\Delta f(\varepsilon(n))}{(\omega)^2 - (\Delta)^2}. \tag{13}$$

Next, we consider the coefficient $C_{nn'}(x)$ in equation (10) and expand it to lowest order in its argument (low wavenumber expansion). In this case, we are only considering the $n' = n \pm 1$ terms. The inter-Landau-band plasmon modes under consideration arise from neighbouring Landau bands. Hence for $n' = n + 1$ and $x \ll 1$, using the following associated Laguerre polynomial expansion $L_n^l(x) = \sum_{m=0}^{n}(-1)^m \frac{(n+l)!}{(l+m)!(n-m)!}\frac{x^m}{m!}$ for $l > 0$ [23] and retaining the first term in the expansion for $x \ll 1$, $C_{nn'}(x)$ reduces to

$$C_{n,n+1}(x) \to (n+1)x, \tag{14}$$

and for $n' = n - 1$ and $x \ll 1$ it reduces to

$$C_{n,n-1}(x) \to nx. \tag{15}$$

Substitution of equations (13)–(15) into (10) and replacing $x = \frac{\bar{q}^2}{2eB}$ yields

$$1 = \frac{2\pi e^2}{\kappa\bar{q}}\frac{2}{\pi l^2}\sum_n \left((n+1)\left(\frac{\bar{q}^2}{2eB}\right)\frac{2\left(\frac{\omega_g}{2\sqrt{n}}\right)f(\varepsilon(n))}{\left(\omega^2 - \left(\frac{\omega_g}{2\sqrt{n}}\right)^2\right)} + n\left(\frac{\bar{q}^2}{2eB}\right)\frac{2\left(-\frac{\omega_g}{2\sqrt{n}}\right)f(\varepsilon(n))}{\left(\omega^2 - \left(\frac{\omega_g}{2\sqrt{n}}\right)^2\right)}\right). \tag{16}$$

In obtaining the above result we note that $\Delta = (\sqrt{n'} - \sqrt{n})\omega_g$. Therefore, $\Delta = \frac{\omega_g}{2\sqrt{n}}$ for $n' = n + 1$, and $\Delta = -\frac{\omega_g}{2\sqrt{n}}$ for $n' = n - 1$. We are considering the weak magnetic field case where many Landau levels are filled. In that case, we may substitute $\sqrt{n_F}$ for $\sqrt{n}$ in equation (16). $n_F = (\frac{\varepsilon_F}{\omega_g})^2$ is the Landau level index corresponding to the Fermi energy ε_F. Equation (16) can be expressed as

$$\omega^2 = \frac{2\pi e^2 v_F}{\kappa}\bar{q}\left(\sum_n \frac{2eB}{\pi k_F} f(\varepsilon(n))\right). \tag{17}$$

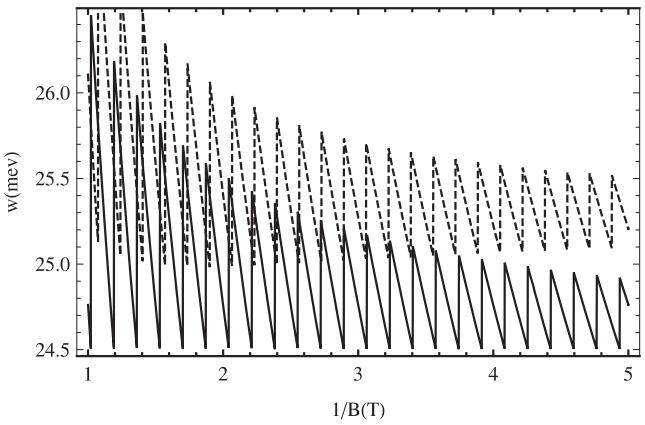

Figure 1. Inter-Landau-band magnetoplasmon energy as a function of inverse magnetic field: graphene monolayer (solid curve), 2DEG (dashed curve). The dashed curve has been scaled by 4.2×.

In terms of the 2D electron density $n_{2D} = \sum_n \frac{2eB}{\pi} f(\varepsilon_n)$ the inter-Landau-band plasmon dispersion relation for monolayer graphene can be expressed as

$$\omega^2 = \frac{2\pi e^2 v_F n_{2D}}{\kappa k_F}\bar{q}. \tag{18}$$

A corresponding calculation for bilayer graphene can be carried out. The equation that replaces equation (16), given above for monolayer graphene, is

$$1 = \frac{2\pi e^2}{\kappa\bar{q}}\frac{2}{\pi l^2}\sum_n \left((n+1)\left(\frac{\bar{q}^2}{2eB}\right)\frac{2(\omega_b)f(\varepsilon_n)}{(\omega^2 - (\omega_b)^2)} + n\left(\frac{\bar{q}^2}{2eB}\right)\frac{2(-\omega_b)f(\varepsilon_n)}{(\omega^2 - (\omega_b)^2)}\right). \tag{19}$$

For bilayer graphene, equation (19) can be expressed as

$$1 = \frac{4\pi e^2}{\kappa m^*}\bar{q}\frac{1}{\omega^2 - (\omega_b)^2}\left(\frac{m^*\omega_b}{\pi}\sum_n f(\varepsilon_n)\right). \tag{20}$$

If we define $n_{2D} = \frac{m^*\omega_b}{\pi}\sum_n f(\varepsilon_n)$ and the plasma frequency as

$$\omega_{p,2D}^2 = \frac{4\pi n_{2D} e^2}{\kappa m^*}\bar{q}, \tag{21}$$

then the inter-Landau-band plasmon dispersion relation for bilayer graphene is

$$\omega^2 = (\omega_b)^2 + \omega_{p,2D}^2. \tag{22}$$

3.2. Discussion of results

Equations (18) and (22) are the central results of this work. Equation (18) is the inter-Landau-band plasmon dispersion relation for monolayer graphene. The inter-Landau-band plasmon energy as a function of the inverse magnetic field for the monolayer and bilayer graphene system with the plasmon energy for 2DEG at zero temperature is presented in figures 1 and 2. The following parameters were employed for doped graphene (SiO_2 substrate): $\kappa = 2.5$, $n_{2D} = 3 \times 10^{15}$ m^{-2},

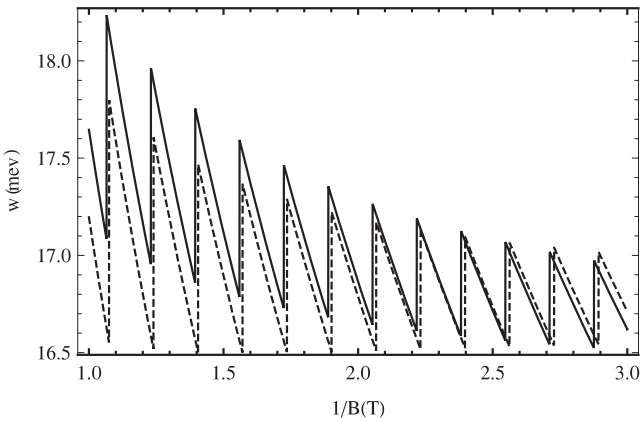

Figure 2. Inter-Landau-band magnetoplasmon energy as a function of inverse magnetic field: graphene bilayer (solid curve), 2DEG (dashed curve). The dashed curve has been scaled by 2.6×.

$v_F = 10^6$ m s^{-1}. For the conventional 2DEG (a 2DEG at the GaAs–AlGaAs heterojunction) we use the following parameters: $m = 0.07m_e$ (m_e is the electron mass), $\kappa = 12$ and $n_{2D} = 3 \times 10^{15}$ m^{-2}. For the electron density and magnetic field considered, electrons fill approximately 30 Landau levels, the upper limit in the summation for n_{2D} is taken to be $n = 30$ while the lower limit is $n = 0$. In figure 1 we have plotted the plasmon energy as a function of the inverse magnetic field for both monolayer graphene and a conventional 2DEG. The SdH-type oscillations, which are a result of emptying out of electrons from successive Landau levels when they pass through the Fermi level as the magnetic field is increased, are clearly visible. The amplitude of these oscillations is a monotonic function of the magnetic field. These oscillations have a π Berry's phase due to the chiral nature of the quasiparticles in this system, the phase acquired by Dirac electrons in the presence of a magnetic field [1]. We also observe that the plasmon energy is ∼4.2 times greater than in the 2DEG for the parameters considered. This is essentially due to the higher Fermi energy of the electrons in graphene and the smaller background dielectric constant.

For bilayer graphene, we consider equation (22). There are two main differences between the plasmon dispersion relation for bilayer graphene given in equation (22) and the standard 2DEG result. Firstly, the cyclotron frequency ω_b in the bilayer is ∼2 greater than the cyclotron frequency ω_c at the same magnetic field in the 2DEG due to the difference in the effective masses of the electrons in the two systems. Secondly, the 2D plasma frequency $\omega_{p,2D}$ is also larger than in the 2DEG for the same wavenumber $\bar{q}$ due to the smaller effective mass of electrons in the bilayer compared to the 2DEG and the smaller background dielectric constant $k = 3$ in the bilayer. The inter-Landau-band plasmon energy as a function of the inverse magnetic field for a doped bilayer and the 2DEG is shown in figure 2. The following parameters were used (SiO_2 substrate): $\kappa = 3$, $n_{2D} = 3 \times 10^{15}$ m^{-2} and $m^* = 0.044m_e$ with m_e being the usual electron mass. We again observe SdH-type oscillations whose amplitude is a monotonic function of the magnetic field. We observe that the plasmon energy is ∼2.6 times greater than in the 2DEG due to the smaller effective mass, valley degeneracy and smaller background dielectric constant. Due to the chiral nature of the quasiparticles in bilayer graphene, 2π Berry's phase is evident in the SdH-type oscillations displayed in figure 2. In conclusion, we have determined the inter-Landau-band plasmon frequency for both monolayer and bilayer graphene employing the SCF approach. The inter-Landau-band plasmon energy is presented as a function of the inverse magnetic field. The SdH-type oscillations are clearly visible in both the systems and their amplitude is a monotonic function of the magnetic field. Due to the chiral nature of the quasiparticles in the mono- and bilayer graphene system, π and 2π Berry's phases are observed in the SdH-type oscillations in the plasmon spectrum.

Acknowledgments

One of us (KS) would like to acknowledge the support of the Pakistan Science Foundation (PSF) through project No. C-QU/Phys (129). MT would like to acknowledge the support of the Pakistan Higher Education Commission (HEC).

References

[1] Novoselov K S, Geim A K, Morozov S V, Jiang D, Katsnelson M I, Grigorieva I V, Dubonos S V and Firsov A A 2005 *Nature* **438** 197
Zhang Y, Tan Y W, Stormer H L and Kim P 2005 *Nature* **438** 201
[2] Zheng Y and Ando T 2002 *Phys. Rev.* B **65** 245420
Gusynin V P and Sharapov S G 2005 *Phys. Rev. Lett.* **95** 146801
Perez N M R, Guinea F and Castro Neto A H 2006 *Phys. Rev.* B **73** 125411
Katsnelson M I, Novoselov K S and Geim A K 2006 *Nat. Phys.* **2** 620
Novoselov K S, McCann E, Morozov S V, Fal'ko V I, Katsnelson M I, Zeitler U, Jiang D, Schedin F and Geim A K 2006 *Nat. Phys.* **2** 177
[3] Deacon R S, Chuang K-C, Nicholas R J, Novoselov K S and Geim A K 2007 arXiv:0704.0410v3
Zhou S Y, Gweon G-H, Graf J, Fedorov A V, Spataru C D, Diehl R D, Kopelevich Y, Lee D H, Louie S G and Lanzara A 2006 *Nat. Phys.* **2** 595
[4] Partoens B and Peeters F M 2007 *Phys. Rev.* B **75** 193402
[5] McCann E and Fal'ko V I 2006 *Phys. Rev. Lett.* **96** 086805
Abergel D S L and Fal'ko V I 2007 *Phys. Rev.* B **75** 155430
[6] Wang X-F and Chakarborty T 2007 *Phys. Rev.* B **75** 041404
[7] Henriksen E A, Jiang Z, Tung L-C, Schwartz M E, Takita M, Wang Y-J, Kim P and Stormer H L 2008 *Phys. Rev. Lett.* **100** 087403
[8] Kallin C and Halperin B I 1984 *Phys. Rev.* B **30** 5655
[9] MacDonald A H 1985 *J. Phys. C: Solid State Phys.* **18** 1003
Oji H C A and MacDonald A H 1986 *Phys. Rev.* B **33** 3810
[10] Que W-M and Kirczenow G 1989 *Phys. Rev. Lett.* **62** 1687
[11] Batke E, Heitmann D and Tu C W 1986 *Phys. Rev.* B **34** 6951
[12] Pinczuk A, Valladares J P, Heiman D, Gossard A C, English J H, Tu C W, Pfeiffer L and West K 1988 *Phys. Rev. Lett.* **61** 2701
[13] Pinczuk A, Schmitt-Rink S, Danan G, Valladares J P, Pfeiffer L N and West K 1988 *Phys. Rev. Lett.* **61** 2701
[14] Eriksson M A, Pinczuk A, Dennis B S, Simon S H, Pfeiffer L N and West K 1999 *Phys. Rev. Lett.* **82** 2163
[15] Brozak G, Shanabrook B V, Gammon D and Katzer D S 1993 *Phys. Rev.* B **47** 9981

[16] Apalkov V, Wang X-F and Chakraborty T 2007 *Int. J. Mod. Phys.* B **21** 1167
[17] Hwang E H and Das Sarma S 2007 *Phys. Rev.* B **75** 205418
[18] Wang X-F and Chakraborty T 2007 *Phys. Rev.* B **75** 033408
[19] Shung Kenneth W-K 1986 *Phys. Rev.* B **34** 979
[20] Lin M-F and Shyu F-L 2000 *J. Phys. Soc. Japan* **69** 607
[21] Eberlein T, Bangert U, Nair R R, Jones R, Gass M, Bleloch A L, Novosalev K S, Geim A and Briddon P R 2008 *Phys. Rev.* B **77** 233406
[22] Ehrenreich H and Cohen M H 1959 *Phys. Rev.* **115** 786
[23] Gradshteyn I S and Ryzhik I M 1980 *Table of Integrals, Series and Products* (New York: Academic)